PROCEEDINGS OF SCIENCE

Theoretical discrepancies in the nucleon spin structure and the hyperfine splitting of muonic hydrogen

Vladimir Pascalutsa,[a,*] **Franziska Hagelstein**[a,b] **and Vadim Lensky**[a]

[a] *Johannes-Gutenberg Universität Mainz, D-55099 Mainz, Germany*

[b] *Paul Scherrer Institut, CH-5232 Villigen PSI, Switzerland*

E-mail: hagelste@uni-mainz.de, vlenskiy@uni-mainz.de, pascalut@uni-mainz.de

Two groups, ours (Mainz) and Bochum, have recently been re-evaluating the spin polarizabilities and spin structure functions at low Q, using the baryon chiral perturbation theory (BχPT), the manifestly-covariant counterpart of the heavy-baryon chiral perturbation theory (HBχPT). Whilst the two groups agree that the BχPT framework works better than HBχPT in this sector, their quantitative results disagree in some of the quantities; most notably, the proton spin polarizabilities γ_0 and δ_{LT}. These discrepancies are especially intriguing in light of new experimental data coming from the Jefferson Lab "Spin Physics Program". The preliminary data on the proton are reported by Karl Slifer in a plenary session of this workshop.

Another theoretical discrepancy is emerging in the proton-polarizability contribution to the hyperfine splitting (hfs) in hydrogen and muonic hydrogen. Our BχPT calculation shows a significantly smaller effect than the state-of-the-art data-driven evaluations based on empirical spin structure functions. The smaller polarizability contribution leads to a smaller Zemach radius of the proton. This discrepancy could be relevant for the planned first-ever measurement of the ground-state hfs in muonic hydrogen.

The 10th International Workshop on Chiral Dynamics - CD2021
15-19 November 2021
Online

*Speaker

PoS(CD2021)102

1. Introduction

Compton scattering off nucleons ($\gamma N \to \gamma N$) is one of the simplest processes by which we access the electromagnetic structure of the nucleon. It plays a central role in the calculation of the two-photon-exchange (2γ-exchange) corrections, Fig. 1, in hydrogen (H) and muonic hydrogen (μH), as well as, of the radiative corrections to elastic lepton-nucleon scattering (see, e.g., [1, 2] for reviews).

The description of nucleon structure at low energy relies on data-driven dispersive approaches, lattice QCD, and low-energy effective field theories (EFTs). Here we focus on the latter. We employ the baryon chiral perturbation theory (BχPT) [3–5] — an EFT operating in terms of pion, nucleon and Δ-isobar fields — to compute the forward doubly-virtual Compton scattering (VVCS) on the nucleon at next-to-next-to-leading order [6–8]. An analogous calculation is done by the Bochum group [9, 10], with insofar inexplicable differences to our results (compare, e.g., blue and grey bands in Fig. 2).

The VVCS amplitudes contain the main ingredients of the nucleon electromagnetic structure: form factors, polarizabilities, structure functions, which is useful in evaluations of the aforementioned 2γ-exchange corrections. For example, the nucleon spin structure functions g_1 and g_2 are important for extractions of nuclear Zemach radii from the hyperfine-splitting (hfs) measurements in light muonic atoms. Presently, several collaborations (CREMA [11], FAMU [12, 13] and J-PARC/Riken [14]) are preparing measurements of the ground-state hfs in μH and μ^3He$^+$. These will allow one to extract the Zemach radii of the proton and helion, and learn about their magnetic properties. For a successful measurement, precise theory predictions are needed to narrow down the frequency search range in the experiments, see [15] for review. In light muonic atoms, these predictions are usually limited by the uncertainty of the nuclear- and nucleon-structure effects, which mainly stem from the 2γ-exchange to be discussed in this paper.

The paper is organized as follows. In Sec. 2, we show the BχPT predictions for the nucleon spin polarizabilities and moments of polarized structure functions and compare them to experimental data which have been recently obtained at the Jefferson Lab. In Sec. 3, we discuss the leading-order BχPT predictions of the 2γ-exchange polarizability contributions to the hfs in H and μH, and compare them to data-driven dispersive evaluations. We conclude with a summary and conclusions in Sec. 4.

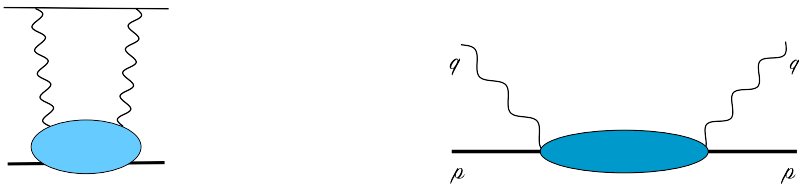

Figure 1: Left: 2γ-exchange diagram; horizontal lines correspond to the lepton and the nucleus (lower, bold). Right: forward Compton scattering.

2. Nucleon Spin Polarizabilities and Moments of Polarized Structure Functions

In the two recent papers [7, 8], we discussed both the spin-independent and spin-dependent VVCS amplitudes, $T_{1,2}(\nu, Q^2)$ and $S_{1,2}(\nu, Q^2)$, functions of the photon energy ν and virtuality Q^2. The absorptive part of these amplitudes, via the optical theorem, yields the unpolarized and polarized structure functions, $\mathrm{Im}\, T_i(\nu, Q^2) \sim F_i(x, Q^2)$ and $\mathrm{Im}\, S_i(\nu, Q^2) \sim g_i(x, Q^2)$, with $x = Q^2/(2M_N\nu)$ the Bjorken variable and M_N the nucleon mass. Here we will focus on the polarized observables, some of which have recently received new experimental data.

The nucleon spin structure functions are being measured at Jefferson Lab within the "Spin Physics Program" [16]. Some new results have been presented in this workshop (see, e.g. [17] and the plenary contribution of K. Slifer). At least three different experiments have recently been mapping out the spin structure functions of the nucleon over a wide kinematic range: the EG4 experiments by the CLAS Collaboration (E03-006 for the proton and E06-017 for the neutron using NH_3 and ND_3 targets) [18, 19], the E97-110 experiment (using a ^{3}He target to study the neutron) [20, 21], and the E08-027 or g2p experiment (using an NH_3 target to study the proton) [22, 23].

We consider, first of all, the following spin polarizabilities:

$$\gamma_0(Q^2) = \frac{16\alpha M_N^2}{Q^6}\int_0^{x_0} \mathrm{d}x\, x^2\left[g_1(x,Q^2) - \frac{4M_N^2x^2}{Q^2}\, g_2(x,Q^2)\right], \tag{1a}$$

$$\delta_{LT}(Q^2) = \frac{16\alpha M_N^2}{Q^6}\int_0^{x_0} \mathrm{d}x\, x^2\left[g_1(x,Q^2) + g_2(x,Q^2)\right], \tag{1b}$$

where $\alpha \simeq 1/137.036$ is the fine structure constant, and x_0 is the inelastic threshold. They are shown in Fig. 2 for the proton (upper panels) and neutron (lower panels). The red curves show the leading, $O(p^3)$ prediction of BχPT (see the Feynman diagrams in Fig. 1 of Ref. [6]). The blue curves and error bands show the next-to-leading, $O(p^{7/2})$ prediction, which includes in addition the $\Delta(1232)$-isobar contributions (Fig. 2 of Ref. [6]). The gray bands show the analogous BχPT calculation by the Bochum group [9]. Apparently there is a significant discrepancy between the two BχPT calculations, especially in the proton δ_{LT}.

Other theory predictions seen in the figure include the considerably older HBχPT calculations. They demonstrate the poor convergence of HBχPT for these quantities (some of the curves are outside the scale of the figure). The pink bands represent the calculation in "infrared regularization" scheme of BχPT, exhibiting unphysical singularities which make it even less viable than HBχPT.

Coming back to the discrepancy between the two BχPT calculations, let us note that one of them (blue bands) comes out to be fairly consistent with the empirical evaluation of MAID [27], represented by the dotted curves in the figure. MAID uses cross sections for individual channels, rather than the total inclusive. However, the integral over x for these quantities converges very rapidly for low x (high energies), which makes the contribution of other channels negligible. Conversely, any large deviation from MAID, as seen, for example, by the Bochum calculation (grey bands) for the proton, should be reproduced by large high-energy contributions on the side of data-driven evaluations.

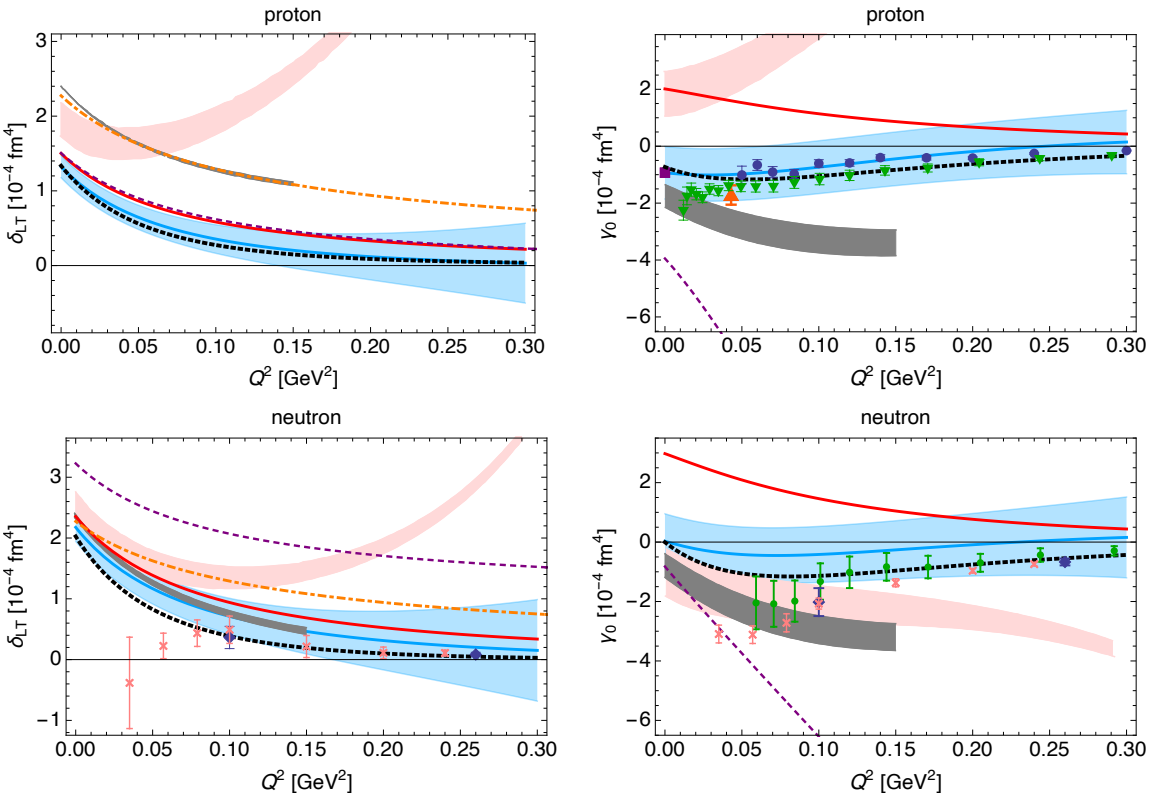

Figure 2: Left: longitudinal-transverse spin polarizability $\delta_{LT}(Q^2)$. Right: forward spin polarizability $\gamma_0(Q^2)$. Upper: proton. Lower: neutron. The red curves represent the $\mathcal{O}(p^3)$ BχPT. The orange dot-dashed and purple dashed curves represent, respectively, $\mathcal{O}(p^3)$ and $\mathcal{O}(p^4)$ HBχPT [24, 25]. The pink bands represent the IR-χPT [26]. The gray bands represent the Bochum BχPT [9]. Our BχPT results [8] are shown by the blue band. The black-dotted curves represent the MAID model with $\pi, \eta, \pi\pi$ channels [27]. Data-driven evaluations: [28] blue dots, [29] purple square for $\gamma_0(0)$, [22] orange pyramid, [19] green triangles, [30] blue diamonds, [31] green dots, and [21] pink crosses.

In this regard, it is interesting to consider the following integrals,

$$I_1(Q^2) = \frac{2M_N^2}{Q^2}\int_0^{x_0} \mathrm{d}x\, g_1(x,Q^2), \tag{2a}$$

$$I_A(Q^2) = \frac{2M_N^2}{Q^2}\int_0^{x_0} \mathrm{d}x \left[g_1(x,Q^2) - \frac{4M_N^2 x^2}{Q^2}\, g_2(x,Q^2)\right]. \tag{2b}$$

These are generalizations of the GDH sum rule. The latter holds at the real-photon point: $I_1(0) = I_A(0) = -\frac{1}{4}\kappa_N$, with κ_N being the nucleon anomalous magnetic moment. The high-energy (low-x) contributions in these integrals are not suppressed by the factor x^2, and hence, the differences with MAID seen in polarizabilities should be amplified here. Certainly, MAID is missing here the higher-energy contributions needed to saturate the GDH sum rule, as is clearly seen at $Q^2 = 0$ in Fig. 3. Yet, these missing contributions are not very large; of the order of tens of percent. Deviations from MAID by factors 2 or 3, seen by the Bochum calculations in Fig. 3, are hardly explainable. Even less so are the large deviations in polarizabilities in Fig. 2, especially in δ_{LT} of the proton.

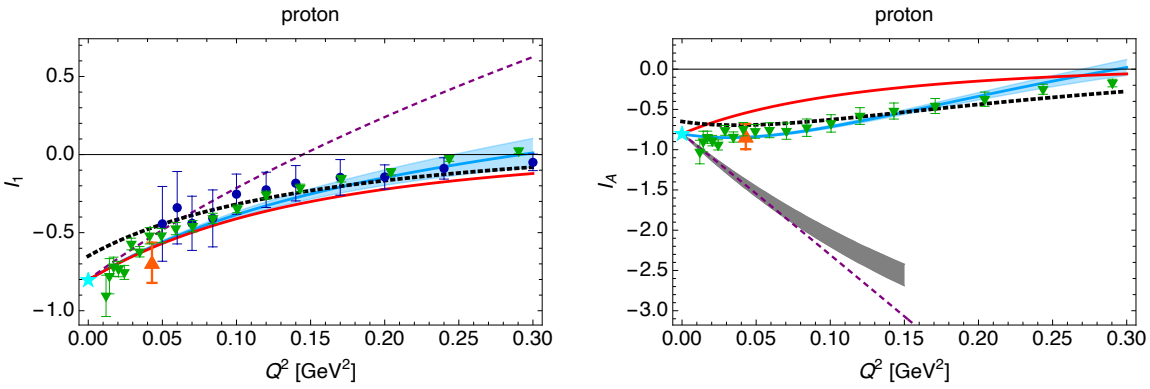

Figure 3: Generalized GDH integrals $I_1(Q^2)$ and $I_A(Q^2)$ of the proton. Legend is the same as in Fig. 2. Data-driven evaluation: The cyan star at $Q^2 = 0$ is the GDH value: $-1/4\kappa_p^2$, using $\kappa_p \approx 1.793$.

The same sentiment applies to the new data-driven evaluation of neutron polarizabilities by the E97-110 Collaboration [21], shown in Fig. 2 by pink crosses. It has anomalously large deviations from MAID in the low-Q region. The new CLAS results for the proton [19] (green triangles) are, on the other hand, more reasonable. Hence, the anomalous results for the neutron is likely due to complications arising in extracting the neutron properties from "neutron targets", e.g., the deuteron or helium-3.

New data for the proton from the g2p Collaboration, presented at this workshop, have sofar been shown in a preprint [23]; see Figs. 2 and 4 therein, for a comparison of theory predictions and data for the proton $\delta_{LT}(Q^2)$ and the inelastic moment $\bar{d}_2(Q^2)$. The latter is defined as:

$$\bar{d}_2(Q^2) = \int_0^{x_0} \mathrm{d}x\, x^2 \,[3g_2(x,Q^2) + 2g_1(x,Q^2)], \tag{3}$$

and relates to the inelastic part of the twist-3 part of the spin structure function $g_2(x,Q^2)$ [32, 33]. Note that this quantity can be derived from the aforementioned quantities, e.g.,

$$\bar{d}_2(Q^2) = \frac{Q^6}{8\alpha M_N^2}\delta_{LT}(Q^2) + \frac{Q^4}{8\alpha M_N^4}\big[I_1(Q^2) - I_A(Q^2)\big], \tag{4}$$

and hence does not add anything new to this discussion.

3. Polarizability Contribution to the Hyperfine Splitting in (Muonic-)Hydrogen

The hfs of the nS-level is proportional to the leading order-α^4 Fermi energy:

$$E_{\rm F} = \frac{8\,\alpha^4 m_r^3}{3mM}(1+\kappa_p), \tag{5}$$

where M is the proton mass, κ_p is the anomalous magnetic moment of the proton, m is the electron or muon mass in the case of H or μH, respectively, and $m_r = mM/(m+M)$ is the reduced mass. The nuclear finite-size effects start contributing at the order α^5, through the forward 2γ exchange, Fig. 1,

which is conventionally split into the elastic (Zemach-radius and recoil) and inelastic (polarizability) contributions [34]:

$$E_{\rm hfs}^{2\gamma}(nS) = \frac{E_{\rm F}}{n^3}\left(\Delta_{\rm Z} + \Delta_{\rm recoil} + \Delta_{\rm pol}\right). \tag{6}$$

The finite-size contributions are obtained from the proton electromagnetic form factors, see, e.g., Ref. [35] for a recent update of the recoil contribution.

The polarizability contribution to hfs is expressed in terms of the spin structure functions:

$$\Delta_{\rm pol} = \Delta_1 + \Delta_2 = \frac{\alpha m}{2\pi(1+\kappa_p)M}\left[\delta_1 + \delta_2\right], \tag{7a}$$

where Δ_1 and Δ_2 are related to the spin-dependent structure functions g_1 and g_2, respectively:

$$\delta_1 = 2\int_0^\infty {\rm d}Q\left(k_0(Q^2)\left[4I_1(Q^2) + F_2^2(Q^2)\right] + \int_0^{x_0} {\rm d}x\, k_1(x,Q^2)\, g_1(x,Q^2)\right), \tag{7b}$$

$$\delta_2 = \int_0^\infty {\rm d}Q \int_0^{x_0} {\rm d}x\, k_2(x,Q^2)\, g_2(x,Q^2), \tag{7c}$$

and the kinematic functions k_i can be found in, e.g., [15]. In Eq. (7b), we isolated the polarizability part, $I_1^{\rm (pol)} = I_1(Q^2) + {}^1\!/\!_4 F_2^2(Q^2)$, of the first moment of the g_1 spin structure function. This is not required to achieve convergence in the dispersive description of the S_1 amplitude. However, it is important because $4I_1(Q^2)$ and $F_2(Q^2)$ cancel exactly at $Q^2 = 0$, thanks to the GDH sum rule. A large cancellation persists also at finite momentum transfer. With the Pauli form factor F_2 and g_1 structure function parametrizations of Refs. [36] and [37], we find contributions to $\Delta_{\rm pol}$ of 1089 ppm and −855 ppm, respectively. Their cancellation into 234 ppm is a considerable source of uncertainty in the data-driven evaluation. Evaluations of the full polarizability contribution, based on similar parametrizations, yield $\Delta_{\rm pol}$ more than a factor 2 smaller than the individual $I_1(Q^2)$ and $F_2(Q^2)$ contributions. A low-Q expansion of Δ_1 is conventionally used to interpolate between the real-photon limit, described by the static values of the forward spin polarizability γ_0 and the anomalous magnetic moment κ, and the onset of data for the g_1 structure function, see, e.g., Ref. [34].

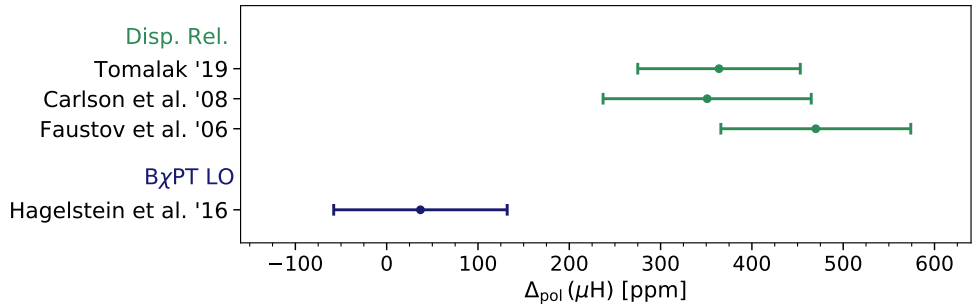

Figure 4: Comparison of predictions for the polarizability contribution to the hfs μH [38–40].

Presently, there is a discrepancy between the data-driven dispersive evaluations and the BχPT predictions of the polarizability contributions to the hfs in μH, see Fig. 4. Similar discrepancy exists in H. The BχPT prediction is considerably smaller and is, in fact, comparable with 0 [41]. This can be understood from a low-energy expansion of the spin-dependent VVCS amplitudes in

the heavy-baryon (HB) limit [42], where the leading HB term, $O(1/m_\pi^2)$, cancels out in $\overline{S}_1(0,Q^2)$. Therefore, the chiral loops in the hfs are essentially vanishing, where the small number is just a remnant of higher orders in the HB expansion.

Since the total 2γ contribution is well constrained by the precise measurement of hydrogen hfs, the smaller polarizability effect in BχPT implies a smaller Zemach radius, cf. the blue band in Fig. 5 and Ref. [15] for more details.

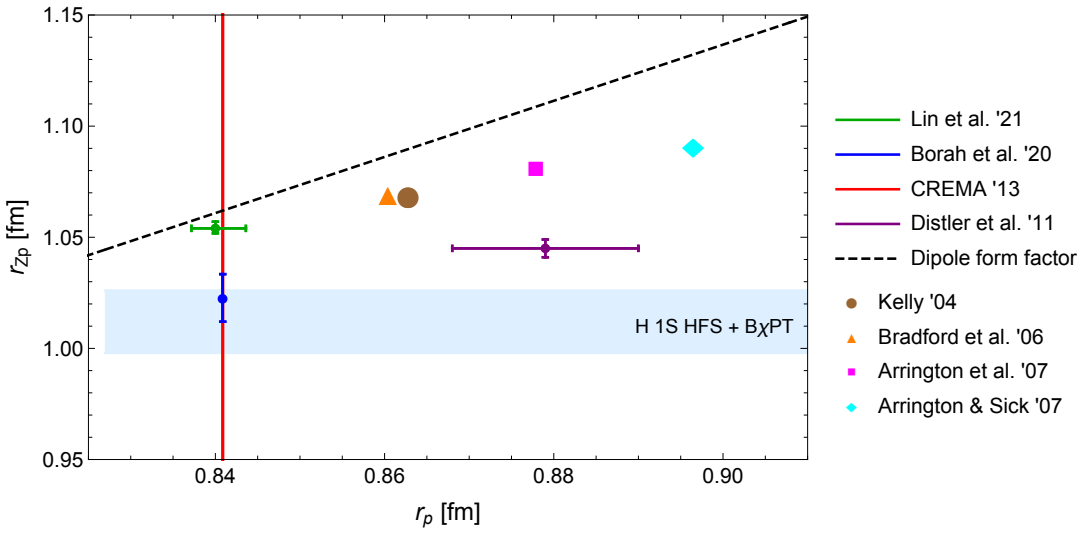

Figure 5: Correlation between the Zemach and charge radius of the proton. The points are from: Lin et al. [43], Borah et al. [44], CREMA [45], Distler et al. [46], Kelly [36], Bradford et al. [47], Arrington et al. [48], and Arrington & Sick [49]. Figure is taken from [15].

4. Conclusion

We have discussed two discrepancies in the current description of the nucleon spin structure at low energies.

- The discrepancy between the two BχPT calculations (Mainz vs. Bochum) of the nucleon spin polarizabilities δ_{LT} and γ_0, and generalized GDH integrals.
- The discrepancy between BχPT and data-driven evaluations of the proton polarizability contribution to hfs, see Fig. 4.

To resolve these discrepancies one does not necessarily need new experimental data, there are plenty of data against which these calculations have not been tested yet.

For example, there is a wealth of empirical information on real Compton scattering of the proton. In the forward kinematics everything is known [29, 50], the value of $\gamma_0(0)$, seen in Fig. 2, is only one of the data points. The off-forward Compton scattering has also been well-measured and can serve as a test of these calculations, see e.g., [51].

The data-driven evaluations of the polarizability contribution to the hyperfine splitting ought to set some benchmarks as well. They could, for example, compute the proton spin polarizabilities and the aforementioned GDH integrals using the same ingredients.

The forthcoming re-analysis of $g_2(x, Q^2)$, and its contribution to hfs, by the g2p Collaboration is promising to improve the situation [22, 23]. They, first of all, obtain new data for this otherwise scarcely-known spin structure function. And they will provide the results for the spin polarizabities and their hfs contribution in the same evaluation.

Acknowledgments

This work is supported by the Swiss National Science Foundation (SNSF) through the Ambizione Grant PZ00P2_193383, the Deutsche Forschungsgemeinschaft (DFG) through the Emmy Noether Programme under the grant 449369623 and through the project 204404729-SFB1044.

References

[1] F. Hagelstein, R. Miskimen and V. Pascalutsa, *Nucleon Polarizabilities: from Compton Scattering to Hydrogen Atom*, *Prog. Part. Nucl. Phys.* **88** (2016) 29 [1512.03765].

[2] B. Pasquini and M. Vanderhaeghen, *Dispersion Theory in Electromagnetic Interactions*, *Ann. Rev. Nucl. Part. Sci.* **68** (2018) 75 [1805.10482].

[3] J. Gasser, M.E. Sainio and A. Svarc, *Nucleons with Chiral Loops*, *Nucl. Phys.* **B 307** (1988) 779.

[4] T. Fuchs, J. Gegelia, G. Japaridze and S. Scherer, *Renormalization of relativistic baryon chiral perturbation theory and power counting*, *Phys. Rev.* **D68** (2003) 056005 [hep-ph/0302117].

[5] V. Pascalutsa and D.R. Phillips, *Effective theory of the delta(1232) in compton scattering off the nucleon*, *Phys. Rev.* **C 67** (2003) 055202 [nucl-th/0212024].

[6] V. Lensky, J.M. Alarcón and V. Pascalutsa, *Moments of nucleon structure functions at next-to-leading order in baryon chiral perturbation theory*, *Phys. Rev.* **C 90** (2014) 055202 [1407.2574].

[7] J.M. Alarcón, F. Hagelstein, V. Lensky and V. Pascalutsa, *Forward doubly-virtual Compton scattering off the nucleon in chiral perturbation theory: the subtraction function and moments of unpolarized structure functions*, *Phys. Rev. D* **102** (2020) 014006 [2005.09518].

[8] J.M. Alarcón, F. Hagelstein, V. Lensky and V. Pascalutsa, *Forward doubly-virtual Compton scattering off the nucleon in chiral perturbation theory: II. Spin polarizabilities and moments of polarized structure functions*, *Phys. Rev. D* **102** (2020) 114026 [2006.08626].

[9] V. Bernard, E. Epelbaum, H. Krebs and U.G. Meißner, *New insights into the spin structure of the nucleon*, *Phys. Rev.* **D 87** (2013) 054032 [1209.2523].

[10] M. Thürmann, E. Epelbaum, A.M. Gasparyan and H. Krebs, *Nucleon polarizabilities in covariant baryon chiral perturbation theory with explicit Δ degrees of freedom*, *Phys. Rev. C* **103** (2021) 035201 [2007.08438].

[11] P. Amaro et al., *Laser excitation of the 1s-hyperfine transition in muonic hydrogen*, 2112.00138.

[12] C. Pizzolotto et al., *Measurement of the muon transfer rate from muonic hydrogen to oxygen in the range 70-336 K*, *Phys. Lett. A* **403** (2021) 127401 [2105.06701].

[13] C. Pizzolotto et al., *The FAMU experiment: muonic hydrogen high precision spectroscopy studies*, *Eur. Phys. J. A* **56** (2020) 185.

[14] M. Sato et al., *Laser spectroscopy of the hyperfine splitting energy in the ground state of muonic hydrogen*, in *Proceedings, 20th International Conference on Particles and Nuclei (PANIC 14), Hamburg, Germany, August 24-29, 2014*, 2014, DOI.

[15] A. Antognini, F. Hagelstein and V. Pascalutsa, *The proton structure in and out of muonic hydrogen*, 2205.10076.

[16] J.P. Chen, *Highlights and Perspectives of the JLab Spin Physics Program*, *Eur. Phys. J. ST* **162** (2008) 103 [0804.4486].

[17] A. Deur, *Results on spin sum rules and polarizabilities at low Q^2*, in *10th International workshop on Chiral Dynamics*, 2, 2022 [2202.10511].

[18] CLAS collaboration, *Measurement of the Q^2 Dependence of the Deuteron Spin Structure Function g_1 and its Moments at Low Q^2 with CLAS*, *Phys. Rev. Lett.* **120** (2018) 062501 [1711.01974].

[19] CLAS collaboration, *Measurement of the proton spin structure at long distances*, *Nature Phys.* **17** (2021) 736 [2102.02658].

[20] Jefferson Lab E97-110 collaboration, *Measurement of the ^{3}He spin-structure functions and of neutron (^{3}He) spin-dependent sum rules at $0.035 \leq Q^2 \leq 0.24$ GeV^2*, *Phys. Lett. B* **805** (2020) 135428 [1908.05709].

[21] E97-110 collaboration, *Puzzle with the precession of the neutron spin*, *Nature Phys.* **17** (2021) 687 [2103.03333].

[22] R. Zielinski, *The g2p Experiment: A Measurement of the Proton's Spin Structure Functions*, Ph.D. thesis, New Hampshire U., 2017. 1708.08297.

[23] Jefferson Lab Hall A g2p collaboration, *The Proton Spin Structure Function g_2 and Generalized Polarizabilities in the Strong QCD Regime*, 2204.10224.

[24] C.W. Kao, T. Spitzenberg and M. Vanderhaeghen, *Burkhardt-Cottingham sum rule and forward spin polarizabilities in heavy baryon chiral perturbation theory*, *Phys. Rev.* **D 67** (2003) 016001 [hep-ph/0209241].

[25] C.-W. Kao, D. Drechsel, S. Kamalov and M. Vanderhaeghen, *Higher moments of nucleon spin structure functions in heavy baryon chiral perturbation theory and in a resonance model*, *Phys. Rev.* **D 69** (2004) 056004 [hep-ph/0312102].

[26] V. Bernard, T.R. Hemmert and U.-G. Meißner, *Spin structure of the nucleon at low energies*, *Phys. Rev.* **D 67** (2003) 076008 [hep-ph/0212033].

[27] D. Drechsel, B. Pasquini and M. Vanderhaeghen, *Dispersion relations in real and virtual Compton scattering*, *Phys. Rept.* **378** (2003) 99 [hep-ph/0212124].

[28] CLAS collaboration, *Moments of the Spin Structure Functions g_1^p and g_1^d for $0.05 < Q^2 < 3.0$ GeV^2*, *Phys. Lett.* **B 672** (2009) 12 [0802.2232].

[29] O. Gryniuk, F. Hagelstein and V. Pascalutsa, *Evaluation of the forward Compton scattering off protons: II. Spin-dependent amplitude and observables*, *Phys. Rev.* **D 94** (2016) 034043 [1604.00789].

[30] Jefferson Lab E94010 collaboration, *Measurement of the generalized forward spin polarizabilities of the neutron*, *Phys. Rev. Lett.* **93** (2004) 152301 [nucl-ex/0406005].

[31] CLAS collaboration, *Precise determination of the deuteron spin structure at low to moderate Q^2 with CLAS and extraction of the neutron contribution*, *Phys. Rev. C* **92** (2015) 055201 [1505.07877].

[32] R. Jaffe, *g_2–The nucleon's other spin-dependent structure function*, *Comments Nucl. Part. Phys.* **19** (1990) 239.

[33] E.V. Shuryak and A. Vainshtein, *Theory of power corrections to deep inelastic scattering in quantum chromodynamics: (II). Q^{-4} effects; polarized target*, *Nucl. Phys. B* **201** (1982) 141.

[34] C.E. Carlson, V. Nazaryan and K. Griffioen, *Proton structure corrections to electronic and muonic hydrogen hyperfine splitting*, *Phys. Rev.* **A 78** (2008) 022517 [0805.2603].

[35] A. Antognini, Y.-H. Lin and U.-G. Meißner, *Precision calculation of the recoil–finite-size correction for the hyperfine splitting in muonic and electronic hydrogen*, 2208.04025.

[36] J.J. Kelly, *Simple parametrization of nucleon form factors*, *Phys. Rev.* **C 70** (2004) 068202.

[37] S. Simula, M. Osipenko, G. Ricco and M. Taiuti, *Leading and higher twists in the proton polarized structure function g**p(1) at large Bjorken x*, *Phys. Rev.* **D 65** (2002) 034017 [hep-ph/0107036].

[38] C.E. Carlson, V. Nazaryan and K. Griffioen, *Proton structure corrections to hyperfine splitting in muonic hydrogen*, *Phys. Rev.* **A 83** (2011) 042509 [1101.3239].

[39] R. Faustov, I. Gorbacheva and A. Martynenko, *Proton polarizability effect in the hyperfine splitting of the hydrogen atom*, *Proc. SPIE Int. Soc. Opt. Eng.* **6165** (2006) 0M [hep-ph/0610332].

[40] O. Tomalak, *Two-Photon Exchange Correction to the Lamb Shift and Hyperfine Splitting of S Levels*, *Eur. Phys. J. A* **55** (2019) 64 [1808.09204].

[41] F. Hagelstein and V. Pascalutsa, *Proton structure in the hyperfine splitting of muonic hydrogen*, *PoS* **CD15** (2016) 077 [1511.04301].

[42] A. Pineda, *Leading chiral logs to the hyperfine splitting of the hydrogen and muonic hydrogen*, *Phys. Rev. C* **67** (2003) 025201 [hep-ph/0210210].

[43] Y.-H. Lin, H.-W. Hammer and U.-G. Meißner, *New Insights into the Nucleon's Electromagnetic Structure*, *Phys. Rev. Lett.* **128** (2022) 052002 [2109.12961].

[44] K. Borah, R.J. Hill, G. Lee and O. Tomalak, *Parameterization and applications of the low-Q^2 nucleon vector form factors*, *Phys. Rev. D* **102** (2020) 074012 [2003.13640].

[45] A. Antognini, F. Nez, K. Schuhmann, F.D. Amaro et al., *Proton Structure from the Measurement of $2S-2P$ Transition Frequencies of Muonic Hydrogen*, *Science* **339** (2013) 417.

[46] M.O. Distler, J.C. Bernauer and T. Walcher, *The RMS Charge Radius of the Proton and Zemach Moments*, *Phys. Lett.* **B 696** (2011) 343 [1011.1861].

[47] R. Bradford, A. Bodek, H.S. Budd and J. Arrington, *A New parameterization of the nucleon elastic form-factors*, *Nucl. Phys. Proc. Suppl.* **159** (2006) 127 [hep-ex/0602017].

[48] J. Arrington, W. Melnitchouk and J.A. Tjon, *Global analysis of proton elastic form factor data with two-photon exchange corrections*, *Phys. Rev.* **C 76** (2007) 035205 [arXiv:0707.1861 [nucl-ex]].

[49] J. Arrington and I. Sick, *Precise determination of low-Q nucleon electromagnetic form factors and their impact on parity-violating e-p elastic scattering*, *Phys. Rev.* **C 76** (2007) 035201 [nucl-th/0612079].

[50] O. Gryniuk, F. Hagelstein and V. Pascalutsa, *Evaluation of the forward Compton scattering off protons: Spin-independent amplitude*, *Phys. Rev. D* **92** (2015) 074031 [1508.07952].

[51] V. Lensky, J. McGovern and V. Pascalutsa, *Predictions of covariant chiral perturbation theory for nucleon polarisabilities and polarised Compton scattering*, *Eur. Phys. J.* **C 75** (2015) 604 [1510.02794].

PoS(CD2021)102